

Relaxing in foam

A.D. Gopal and D.J. Durian

UCLA Department of Physics & Astronomy, Los Angeles, CA 90095-1547

(Dated: March 22, 2022)

We investigate the linear mechanical response of an aqueous foam, and its relation to the microscopic rearrangement dynamics of the bubble-packing structure. At rest, even though the foam is coarsening, the rheology is demonstrated to be linear. Under flow, shear-induced rearrangements compete with coarsening-induced rearrangements. The macroscopic consequences are captured by a novel rheological method in which a step-strain is superposed on an otherwise steady flow.

PACS numbers: 82.70.Rr, 83.60.Rs, 83.80.Iz, 83.85.Cg

Aqueous foams are tightly packed collections of gas bubbles separated by a continuous liquid phase [1, 2]. Like elastic solids, bulk foams resist shear, completely unlike the gases and liquids from which they are comprised. The origin of this striking behavior is that the bubbles are jammed, unable to flow around one another and explore configuration space under thermal energy. Thus bubbles distort, rather than rearrange, when subjected to small shear deformations. The resulting extra internal gas-liquid surface area costs energy in proportion to the surface tension, and this provides a restoring force. The shear modulus is roughly surface tension divided by bubble radius, depending precisely on the volume fraction, ε , of the continuous liquid phase [3, 4, 5]. As a foam is made wetter, the bubbles become progressively rounder, and the shear modulus decreases. The elasticity completely vanishes at the point where the bubbles are close-packed spheres. This is one example of unjamming [6].

In this paper we explore other ways to unjam the bubbles in a foam. Each could correspond to a different trajectory in a global jamming phase diagram [7]. For example, one could imagine raising the temperature so that $k_B T$ is greater than σR^2 , which would allow the bubbles to rearrange thermally like Brownian particles. However, a typical value is $\sigma R^2/k_B \approx 10^{12}$ K; therefore, foams are athermal far-from-equilibrium systems and raising the temperature is not feasible. But there are at least two other ways to drive the system so that bubble rearrangements occur. One is through coarsening, the diffusion of gas from smaller to larger bubbles. As this proceeds, local stress inhomogeneities repeatedly build up to some threshold and relax by sudden avalanche-like local rearrangements. Such microscopic dynamics have been observed previously via diffusing-wave spectroscopy (DWS) [8, 9, 10]. This raises a string of interesting questions. How do localized coarsening-induced rearrangements affect the linear shear rheology of bulk foams? Is the effect similar to thermally excited dynamic heterogeneities in glassy systems? An entirely different way to induce rearrangements is by shear. Here local stresses also accrue and relax, but in a more correlated manner. These rearrangement dynamics have similarly been studied by DWS

[11, 12, 13]. How does the elastic character of foam vanish as the shear rate is increased? Can we think of the two driving mechanisms as “heating” and ultimately unjamming the sample? To make progress, we study the linear mechanical response of an aqueous foam at very long times and low frequencies. In a novel twist, we also study linear response *during* uniform shear flow.

Our samples are a commercial aqueous foam, consisting of nearly-spherical polydisperse gas bubbles, 92% by volume, that are tightly packed in an aqueous solution of stearic acid and triethanolamine (Gillette Company, Boston MA). Samples are surrounded by a water bath held at 25.0°C and are measured after the foam has aged for approximately 100 minutes. By this time, the average bubble size is approximately 60 microns and is growing reproducibly via coarsening [14]; stresses due to the loading process have also relaxed. Test durations are sufficiently short that gravitational liquid drainage and bubble coalescence are negligible.

Our measurements are performed with a Paar Physica UDS 200 rheometer, controlling the rotational speed and angular displacement of a solid cylinder whose axis is vertical and concentric with a fixed surrounding cup. The sample cell has an inner radius of 20.0 mm, and a 4.1 mm gap; these dimensions ensure that the foam can be treated as a bulk material with uniform stress. To minimize end-flow effects, the 98 mm long inner cylinder is much shorter than the depth of the surrounding cup yet much longer than the gap width. Wall slip is precluded by coating both the cylinder and cup with a fine-grade sandpaper. Samples are loaded through a 5 mm hole at the bottom of the cup, after lowering the cylinder to the test position. DWS measurements indicate the absence of shear-banding and other secondary flows [13]. To re-confirm, we compared with a similarly coated cone-and-plate cell, with a 10 cm radius and 10° cone angle. Identical rheology results were obtained for both cell configurations, implying that the imposed shear deformation is uniform. Diffuse light transmission indicates that bubbles do not burst, and voids do not form, even under high shear [12, 13].

Effect of coarsening on mechanical response. To quantify linear response, we measure both the complex shear

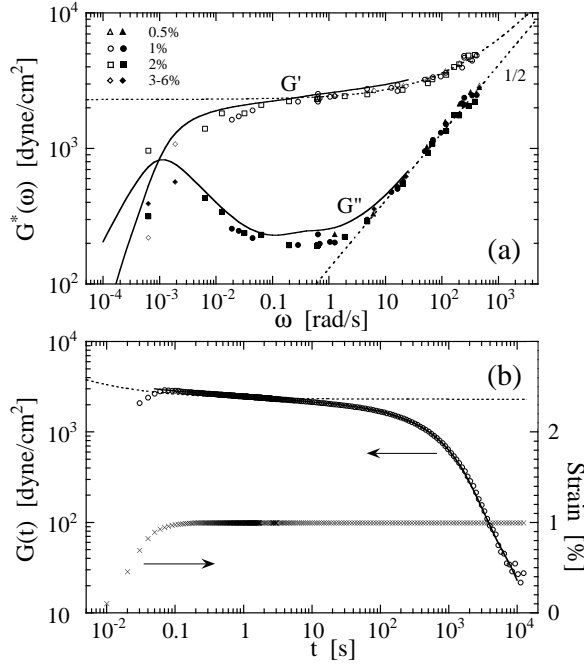


FIG. 1: Dynamic shear moduli of a coarsening foam, in both the (a) frequency and (b) time domains; symbols in (a) denote the imposed strain amplitude. The dashed curves in (a-b) are a fit to $G^*(\omega) = G_o(1 + \sqrt{i\omega/\omega_n})$ and $G(t) = G_o(1 + 1/\sqrt{\pi\omega_n t})$, predicted for nonaffine bubble motion in the absence of any time evolution. The solid curve in (b) is an empirical fit to $G(t)$; appropriately transformed, it gives the solid curves matching the storage and loss moduli in (a).

modulus, $G^*(\omega) = G'(\omega) + iG''(\omega)$ [15, 16], and the stress relaxation modulus, $G(t)$ [15, 16]. Our data are displayed in Fig. 1. Note that $G'(\omega) > G''(\omega)$, meaning that the response is primarily elastic rather than dissipative. The frequency range for our $G^*(\omega)$ data spans almost six decades, from 2π divided by sample age (an absolute minimum below which measurement is not possible) up to a maximum set by limitations of the rheometer. Note that different amplitude strains give the same result, demonstrating absence of wall-slip and other geometry-dependent artifacts and hinting at linearity of response. A more stringent test of linearity is comparison with $G(t)$, which should be related to $G^*(\omega)$ by Fourier transform [15, 16]. The time range for our $G(t)$ data spans over five decades, from the time needed to achieve the step strain up to the time beyond which stress is zero to within instrumental limits. An empirical fit to the $G(t)$ data is shown in Fig. 1(b) by a solid curve; this fit is transformed and plotted in Fig. 1(a) over a frequency range corresponding to the time range of the fit. The agreement is very good, demonstrating conclusively that the sample is linear. This is further supported by an empirical fit to $G^*(\omega)$ data at high- ω and the comparison of its transform with $G(t)$ data at short- t .

Let us now consider the frequency and time depen-

dence of the moduli in Fig. 1. The fit for $\omega > 5$ rad/s is to the form $G^*(\omega) = G_o(1 + \sqrt{i\omega/\omega_n})$ with free parameters $G_o = 2300$ dyne/cm² and $\omega_n = 156$ rad/s. The former represents the static shear modulus, roughly surface tension divided by bubble size [3, 4, 5]. The latter represents the effect of nonaffine deformation of the bubbles under shear due to local packing configurations that are strong or weak with respect to the shear direction [17]. This fit, including the parameters, is consistent with the $G^*(\omega)$ data in Ref. [18], where the frequency range (0.3–20 rad/s) was too small to fully demonstrate the functional form. According to the theory of [17], the characteristic frequency is $\omega_n \propto G_o/\eta_\infty$, where the very-high frequency response is $G^*(\omega) = i\eta_\infty\omega$. The numerical prefactor was not predicted; experimentally, it was found to depend on ε and was not of order 1. To compare, the value is $\omega_n \approx 600$ rad/s for a $\varepsilon = 0.38$ emulsion of 0.5 μm oil droplets in water [17, 19] (NB: by our definition, ω_n may be easily read off a plot by locating where $G'(2\omega_n) = 2G_o$ and $G''(2\omega_n) = G_o$).

The fit to $G_o(1 + \sqrt{i\omega/\omega_n})$ fails for $\omega < 5$ rad/s; the corresponding transform fails for $t > 20$ s. At longer times, the $G(t)$ data decay slowly below G_o , almost logarithmically, over a few decades before relaxing more rapidly at around 1000 s. The transform of this final decay corresponds to the peak in $G''(\omega)$ at 10^{-3} rad/s. At lower frequencies, $G^*(\omega)$ is unmeasurable; but since the integral of $G(t)$ over all time is finite, the very-low frequency behavior is formally $G''(\omega) \propto \omega$ as required by causality [20]. Thus the full frequency-dependence of $G^*(\omega)$ for our foam is truly known and well-behaved. This resolves a long-standing puzzle [20] raised by earlier measurements [18, 19, 21] where $G^*(\omega)$ was roughly constant down to the lowest measured frequencies.

All that remains is to understand the origin of the low- ω / long- t behavior. We contend that evolution of the foam structure by coarsening is responsible. One clue is that the onset of deviation from the high- ω fits corresponds to the time $\tau_{oq} = 20$ s given by DWS for the time between coarsening-induced rearrangements at each site. Another clue is that the final decay of $G(t)$ and, equivalently, the peak in $G''(\omega)$ correspond to the sample age. Since coarsening gives power-law growth, it takes of order the sample age for the structure to completely change. It is interesting that coarsening-induced rearrangements relax microscopic coarsening-induced stress inhomogeneities far more quickly than the relaxation of macroscopically-imposed stress. Rather, the cumulative effect of many rearrangements and a change in bubble size is needed to relax global stress. The net result is a rheology that obeys linear response. This is remarkable given that the microscopic relaxation mechanism isn't thermal motion, but rather evolution. In effect, coarsening unjams the foam, so that at low frequencies the rheology is $G'(\omega) \ll G''(\omega) = \eta\omega$ like an ordinary equilibrium liquid.

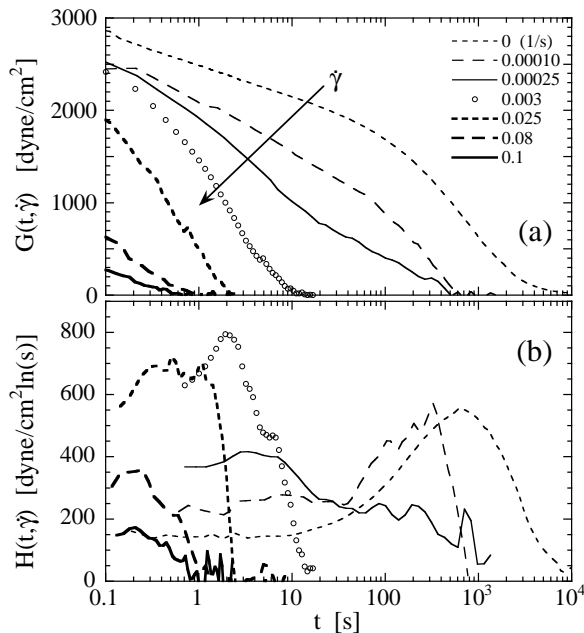


FIG. 2: (a) Stress relaxation moduli for foams sheared at various rates, as listed. This is given from the stress $\sigma(t)$ following the superposition of a step-strain $\Delta\gamma$ on steady shear: $G(t, \dot{\gamma}) = [\sigma(t) - \sigma(0)]/\Delta\gamma$. (b) The corresponding relaxation spectra, $H(t, \dot{\gamma}) \approx dG(t, \dot{\gamma})/d \ln t$.

Effect of shear on mechanical response. Next we investigate how the application of shear causes a similar loss of elasticity. For this we superimpose a small-amplitude step-strain, $\Delta\gamma$, on top of otherwise steady shear at rate $\dot{\gamma}$. The resulting temporary increase in stress defines the transient stress relaxation modulus, $G(t, \dot{\gamma}) = [\sigma(t) - \sigma(0)]/\Delta\gamma$. A frequency-domain version of this technique was developed for polymers [22]. Example data are shown in Fig. 2(a). Note that as the strain rate increases, the elastic character of the foam melts away. There are two signs of this. First, the progressively smaller intercept, $G(0, \dot{\gamma})$, means less elastic energy storage. Second, the progressively shorter decay time means more liquid-like dissipation. At high enough strain rates, where there is no transient storage and only dissipation, the foam behaves like an equilibrium liquid. Similar behavior has now been observed in simulations of a model foam [23].

To further quantify the unjamming behavior apparent in Fig. 2(a), we first deduce the relaxation spectrum, $H(t, \dot{\gamma}) \approx dG(t, \dot{\gamma})/d \ln t$ [15, 16]. Results are shown in Fig. 2(b). For low and zero strain rates, there are two competing relaxation processes, reflected by a broad peak at very late times and long tail of short-time modes of nearly equal weight. The former reflects the coarsening process, and the latter the nonaffine bubble motion. As the shear rate increases, the coarsening peak gradually falls and another peak gradually rises over the nonaffine tail at short times. Presumably this is due to shear-

induced rearrangements.

The salient features of the stress relaxation are shown in Fig. 3 vs strain rate. The first plot is of elastic storage, $G(0, \dot{\gamma})$, the value when the superimposed step-strain is achieved (below about 0.1 s). This decreases very slowly, and is nearly constant, for strain rates less than about 0.05 /s; for higher strain rates it abruptly vanishes. The second plot is of stress relaxation times. One such measure is t_e , when stress falls to $1/e$ of the initial value. Another measure is t_p , where $H(t, \dot{\gamma})$ reaches a global maximum. At zero and very low strain rates, these times are different since there are two competing relaxation mechanisms (evolution and shear). For strain rates higher than about 3×10^{-4} /s, the stress relaxation is essentially exponential and the two relaxation times are hence indistinguishable. In this regime, shear completely dominates the relaxation. It is puzzling that the relaxation time decreases with increasing strain rate as $\dot{\gamma}^{-1/2}$, since on dimensional grounds one would have expected $\dot{\gamma}^{-1}$.

Now we may compare the macroscopic rheology with the nature of the microscopic bubble dynamics. Previously we used DWS to measure the strain rate dependence of two microscopic time scales: τ_o , the time between localized discrete rearrangements, and τ_s , the time for adjacent scattering sites to convect apart by one wavelength of light [13]. The observed DWS data are reproduced by the dashed curves in Fig. 3(b). For very low strain rates, below about 3×10^{-4} /s, the rearrangements are discrete and the time between events, τ_o , is not noticeably different from the quiescent value. The stress relaxation time is much much longer than τ_o - indicating that the cooperative effect of many coarsening-induced rearrangements is required. For slightly higher rates, the time between events decreases, roughly as $\dot{\gamma}^{-1/2}$, just like the stress relaxation time. Since the stress relaxation time is now shorter than τ_o , not every site in the foam must rearrange in order to relax the overall stress. Shear-induced events begin to dominate over coarsening-induced events at strain rates near $\dot{\gamma}_c = \gamma_y/\tau_{oq} = 0.025$ /s, where $\gamma_y = 0.05$ is the yield strain [13]. At still higher rates, events merge together and the flow becomes progressively more homogeneous and smooth. The crossover strain rate is $\dot{\gamma}_m = \gamma_y/\tau_d = 0.5$ /s, where $\tau_d = 0.1$ s is the duration of rearrangements [13]. Many physical quantities display a change in character above and below $\dot{\gamma}_m$ [24]. Indeed, just below $\dot{\gamma}_m$, the new rheological measures of elasticity vanish at precisely where we no longer can detect discrete rearrangements (i.e. at the endpoint of the dashed curve for τ_o). At higher strain rates, the bubble motion is dominated entirely by uniform shear, as characterized by the DWS time scale τ_s . The onset of this correlated shearing motion of bubbles (i.e. the starting point of the τ_s curve) corresponds quite well to where $G(0, \dot{\gamma})$ begins to drop.

Finally, we note that the dramatic changes in the elastic character of the foam with strain rate are not reflected

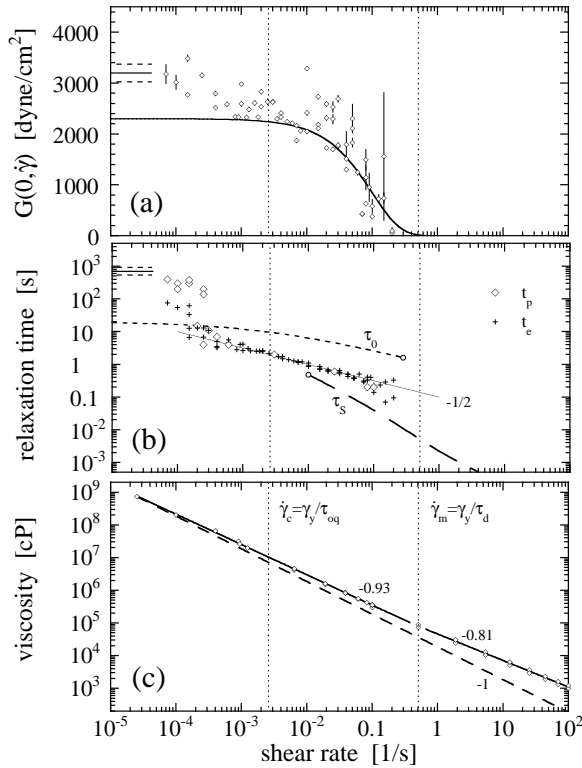


FIG. 3: (a) Transient shear modulus, (b) transient shear relaxation times, and (c) viscosity, all as a function of shear rate. The vertical dotted lines denote the characteristic shear rates set by the yield strain divided respectively by the time between rearrangements and the duration of rearrangements in a quiescent foam. In (a), the solid curve is $G_0 \exp[-\dot{\gamma}/(0.1\text{s}^{-1})]$ where $G_0 = 2300 \text{ dyne/cm}^2$ is the shear modulus. In (b), the open diamonds indicate where $H(t, \dot{\gamma})$ is a global maximum and plusses indicate where $G(t, \dot{\gamma})$ falls to $1/e$ of its initial value; the solid line is a power law with exponent of $-1/2$; the dashed curves indicate DWS time scales for rearrangements (τ_o) and shear (τ_s).

very strongly in the viscosity of the foam. As seen in Fig. 3(c), the viscosity decreases across the whole strain rate range, though not quite as fast as $\dot{\gamma}^{-1}$ (which would have indicated constant stress). There is at most a slight change in exponent at $\dot{\gamma}_m$. Similar behavior is found in simulations [25]. Altogether this emphasizes the importance of the superposition method to measure $G(t, \dot{\gamma})$, since it provides a clear dramatic signature of the unjamming transition. With this tool, and by comparison with DWS data, we have succeeded in connecting the nature of microscopic bubble dynamics with the resulting macroscopic rheological behavior. We have thereby shown that the unjamming of foam can be accomplished both by time and by application of shear. The unjammed liquid-like state is very similar to what would be achieved by raising the temperature for a thermal system. An important next step would be to deduce an effective temper-

ature, recently shown in simulation of a sheared model foam to have many of the attributes of a true statistical mechanical temperature [26].

We thank A.J. Liu and P.T. Mather for helpful discussions. This work was supported by NASA Microgravity Fluid Physics grant NAG3-2481.

-
- [1] R. K. Prud'homme and S. A. Khan, *Foams: Theory, Measurement, and Applications*, vol. 57 of *Surfactant Science Series* (Marcel Dekker, New York, 1996).
 - [2] D. Weaire and S. Hutzler, *The Physics of Foams* (Oxford University Press, New York, 1999).
 - [3] H. M. Princen, J. Coll. I. Sci. **91**, 160 (1983).
 - [4] T. G. Mason, J. Bibette, and D. A. Weitz, Phys. Rev. Lett. **75**, 2501 (1995).
 - [5] A. Saint-Jalmes and D. J. Durian, J. Rheol. **43**, 1411 (1999).
 - [6] A. J. Liu and S. R. Nagel, eds., *Jamming and Rheology* (Taylor and Francis, New York, 2001).
 - [7] A. J. Liu and S. R. Nagel, Nature **396**, 21 (1998).
 - [8] D. J. Durian, D. J. Pine, and D. A. Weitz, Science **252**, 686 (1991).
 - [9] A. D. Gopal and D. J. Durian, J. Opt. Soc. Am. **14**, 150 (1997).
 - [10] S. Cohen-Addad and R. Höhler, Phys. Rev. Lett. **86**, 4700 (2001).
 - [11] J. C. Earnshaw and A. H. Jafaar, Phys. Rev. E **49**, 5408 (1994).
 - [12] A. D. Gopal and D. J. Durian, Phys. Rev. Lett. **75**, 2610 (1995).
 - [13] A. D. Gopal and D. J. Durian, J. Coll. I. Sci. **213**, 169 (1999).
 - [14] D. J. Durian, D. A. Weitz, and D. J. Pine, Science (USA) **252**, 686 (1991).
 - [15] J. D. Ferry, *Viscoelastic Properties of Polymers* (Wiley, New York, 1980), 3rd ed.
 - [16] C. W. Macosko, *Rheology Principles, Measurements, and Applications* (VCH Publishers, New York, 1994).
 - [17] A. J. Liu, S. Ramaswamy, T. G. Mason, and D. A. Weitz, Phys. Rev. Lett. **76**, 3017 (1996).
 - [18] S. Cohen-Addad, H. Hoballah, and R. Höhler, Phys. Rev. E **57**, 6897 (1998).
 - [19] T. G. Mason and D. A. Weitz, Phys. Rev. Lett. **74**, 1250 (1995).
 - [20] D. M. A. Buzza, C.-Y. D. Lu, , and M. E. Cates, J. Phys. II France **5**, 37 (1995).
 - [21] S. A. Khan, A. Schnepfer, and R. C. Armstrong, J. Rheol. **31**, 69 (1988).
 - [22] H. C. Booij, Rheol. Acta **5**, 222 (1966).
 - [23] I. K. Ono, Ph.D. thesis, University of California at Los Angeles (2002).
 - [24] I. K. Ono, S. Tewari, S. A. Langer, and A. J. Liu, submitted to Phys. Rev. E (2002).
 - [25] S. A. Langer and A. J. Liu, Europhys. Lett. **49**, 68 (2000).
 - [26] I. K. Ono, C. S. O'Hern, D. J. Durian, S. A. Langer, A. J. Liu, and S. R. Nagel, Phys. Rev. Lett. **89**, 095703/1 (2002).